# CEBAF PROPOSAL COVER SHEET

This Proposal must be mailed to:

CEBAF
Scientific Director's Office
12000 Jefferson Avenue
Newport News, VA 23606

and received on or before 1 October 1991.

A. TITLE:

Experiments with a polarized $^3$He target and the CEBAF Large Acceptance Spectrometer

B. CONTACT PERSON:

Dr. Robert D. McKeown

ADDRESS, PHONE, AND ELECTRONIC MAIL ADDRESS:

California Institute of Technology
1201 East California Boulevard, 106-38
Pasadena, CA 91125
(818) 356-4316
email BMCK@Caltech

C. IS THIS PROPOSAL BASED ON A PREVIOUSLY SUBMITTED PROPOSAL OR LETTER OF INTENT?

[X] YES [ ] NO

IF YES, TITLE OF PREVIOUSLY SUBMITTED PROPOSAL OR LETTER OF INTENT:

Experiments with a polarized $^3$He target and the CEBAF Large Acceptance Spectrometer

**********

(CEBAF USE ONLY)

Receipt Date 1 OCT 91

Log Number Assigned PR 91-020

By [redacted]

**PROPOSAL TO CEBAF PAC5**
(89-007 Revised)

# Experiments with a polarized $^3$He target and the CEBAF Large Acceptance Spectrometer

*E. Beise, B. Filippone, H. Gao, T. Gentile, W. Lorenzon, and R. McKeown(spokesman)*
W. K. Kellogg Radiation Laboratory
California Institute of Technology
Pasadena, CA 91125

*R. Milner*
Massachusetts Institute of Technology
Cambridge, MA

*J. van den Brand, C. E. Jones*
University of Wisconsin
Madison, WI

*J. R. Calarco, F. W. Hersman*
University of New Hampshire
Durham, NH

*L. Weinstein*
Massachusetts Institute of Technology
Cambridge, MA

*R. Miskimen*
University of Massachusetts
Amherst, MA

*H. Baghaei*
University of Virginia
Charlottesville, VA

and

*V. Burkert, B. Mecking, M. Mestayer, E. Smith, A. Yegneswaran*
CEBAF
Newport News, VA

ABSTRACT

Recent progress in the development of polarized $^3$He targets offers the possibility of performing many new electron scattering experiments using polarized electrons and the CEBAF Large Acceptance Spectrometer (CLAS). We propose to construct a polarized $^3$He target for use with the CLAS and perform measurements of the magnetic and electric form factors of the neutron and small amplitudes in the $^3$He ground state wave-function. These measurements will cover a broad range of momentum transfer ($0.5\ \mathrm{GeV/c^2} \leq Q^2 \leq 2\ \mathrm{GeV/c^2}$) where there is considerable uncertainty in the neutron form factors. The studies of the ground state wave function will allow careful tests of the nuclear structure information necessary for reliable extraction of the neutron form factors. In addition, information on the $\Delta(1232)$ electroproduction amplitudes and the possibility of $\Delta$ amplitudes in the $^3$He ground state will be obtained simultaneously.

## Physics Motivation

Over the last few years, polarized $^3$He targets of sufficient density and polarization to perform interesting electron scattering experiments have been developed.[1] A target of density $2 \times 10^{19}$ atoms/cm$^2$ has been constructed and tested in the 40 $\mu$A electron beam at the Bates laboratory. This target was used to successfully perform the first measurements of the spin-dependent quasielastic nuclear response functions.[2] Thus, the technical feasibility of using polarized $^3$He targets capable of luminosities in the range of $10^{33} - 10^{34}$ cm$^{-2}$s$^{-1}$ with a polarized electron beam at CEBAF has been demonstrated. We propose here a program of measurements aimed at studying both the electromagnetic structure of the neutron at relatively high $Q^2$ and the details of the nuclear wave function of $^3$He. It represents a natural extension of the BLAST program at Bates to higher $Q^2$.

The formalism for electron scattering with spin degrees of freedom has been developed to a point where the physics potential of this technique is now clearly evident.[3] For example, the measurement of the helicity asymmetry with the target spin pointed perpendicular to $\vec{q}$ generally selects structure functions arising from interference between relatively real longitudinal and transverse amplitudes. Many interesting and fundamental physics quantities can be studied by measuring such a structure function. The additional use of final state correlations in coincidence with the electron scattered from a polarized target offers a powerful technique for studying the multipole structure of these interference terms.[4] Such experiments that use the spin degrees of freedom and correlations of final state particles in coincidence with the scattered electron will fully exploit the polarized, high-intensity, CW beam and the large acceptance experimental equipment at CEBAF to perform new fundamental experiments in electronuclear physics. As has been the case in the past, the three-nucleon system offers a unique laboratory for the study of the nucleon and its interactions.

A subject of long-standing interest is the electric form factor of the neutron, $G_E^n$. Our best information at present derives from a rather model-dependent analysis of elastic e-d scattering at low $Q^2$.[5] Recent theoretical work[6] suggests that at higher $Q^2$ the ratio $G_E^n/G_M^n = Q^2/4M^2$ is expected in order to connect with perturbative QCD predictions. CEBAF offers the opportunity to make precision measurements of $G_E^n$ at high $Q^2$ which are of great interest in this context. Polarized $^3$He offers the possibility of studying this quantity in a new way: the $^3$He spin is primarily due to the neutron spin and measurement of the L-T interference enhances the sensitivity to the small longitudinal amplitude which contains the information on $G_E^n$. We thus propose a measurement of $G_E^n$ in quasielastic $\vec{e}$ scattering from polarized $^3$He.

We note that the small amplitudes with the protons in spin $S = 1$ states can be studied in a rather direct fashion using the $(\vec{e}, e'p)$ reaction on a polarized $^3$He target. (In the plane-wave impulse approximation the quasielastic asymmetry would vanish if the protons are in spin $S = 0$ states only.) These amplitudes are of fundamental interest themselves and can be studied in detail using this technique. These data will be obtained simultaneously during the neutron form factor measurements.

The longitudinal C2 amplitude in electroproduction of the $\Delta(1232)$ resonance is of fundamental interest because of its implications for deformation and/or D-waves in the quark structure of the nucleon. This amplitude will be accessible in quasi-free $\Delta$ production

using a polarized $^3$He target.[7]

A more exotic component of the $^3$He ground state wave-function consists of the presence of a $\Delta$ with the other two nucleons coupled to $L = 2$, $S = 0$ and $T = 1$. It was noted by Lipkin and Lee [8] that this component would cause a small anomaly in the ratio of $\pi^+$ to $\pi^-$ production. More recently, Milner and Donnelly [9] have shown that the ratio of *asymmetries* (again $\pi^+/\pi^-$) from polarized $^3$He is much more sensitive to this part of the wave-function: the presence of $\Delta$ components in the ground state with probability of 2% would cause changes in this ratio of order a factor of 2. These data could also be obtained simultaneously with the C2 data.

In this proposal we concentrate our discussion on the neutron form factor measurements along with the coincidence $(e, e'p)$ and $(e, e'n)$ studies of the $^3$He wave function. However, information on these other issues will be obtained simultaneously.

## Quasielastic Scattering from Polarized $^3$He

In this section we present the formalism for quasielastic scattering of longitudinally polarized electrons from polarized $^3$He. Figure 1 shows the kinematics relevant to this process.

The general form for inclusive scattering of longitudinally polarized electrons from a polarized spin 1/2 target is given by[3]

$$\frac{d\sigma}{d\Omega d\omega} = \Sigma \pm \Delta(\theta^*, \phi^*), \tag{1}$$

where $\omega$ is the energy transfer and the angles $\theta^*$ and $\phi^*$ define the target spin direction as shown in figure 1. The plus(minus) sign correspond to positive (negative) helicity incident electrons. The spin-independent cross section $\Sigma$ is given by the usual Rosenbluth formula

$$\Sigma = 4\pi\sigma_{Mott}[v_L R_L(q,\omega) + v_T R_T(q,\omega)], \tag{2}$$

in which $q$ is the momentum tranfer, $v_L$ and $v_T$ are kinematic factors, $R_L$ is the longitudinal response function, and $R_T$ is the transverse response function. These response functions contain the nuclear electromagnetic structure information.

The spin-dependent cross section $\Delta$ contains two new response functions:

$$\Delta = -4\pi\sigma_{Mott}[\cos\theta^* v_{T'} R_{T'}(q,\omega) + 2\sin\theta^* \cos\phi^* v_{TL'} R_{TL'}(q,\omega)]. \tag{3}$$

In particular, the $R_{TL'}$ response function results from interference of longitudinal and transverse amplitudes. Thus it is of special interest in helping to determine longitudinal amplitudes when the transverse amplitudes are dominant. This is the case in quasielastic scattering in $^3$He where $R_{TL'}$ is very sensitive to the value of the neutron electric form factor. On the other hand, the response function $R_{T'}$ in quasielastic scattering from $^3$He is primarily determined by the neutron magnetic form factor.

Experimentally one measures the asymmetry in the cross section under reversal of electron helicity:

$$A \equiv \frac{\Delta}{\Sigma}. \tag{4}$$

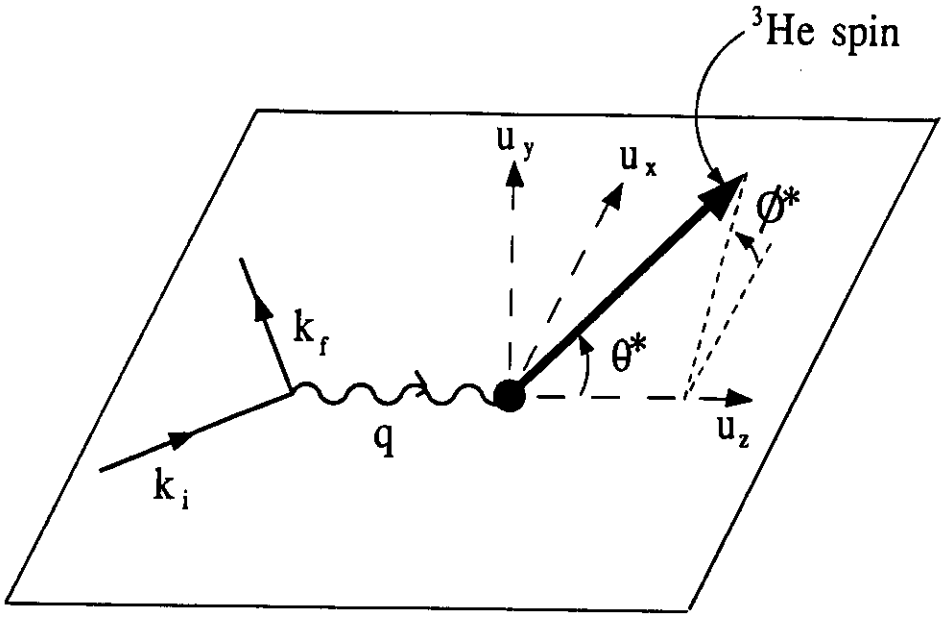


Fig. 1. Kinematic variable definitions for electron scattering from polarized targets. Here $\mathbf{u}_z$ is along the direction of momentum transfer $\mathbf{q}$. The vector $\mathbf{u}_y$ is normal to the electron scattering plane and $\mathbf{u}_x = \mathbf{u}_y \times \mathbf{u}_z$ lies in the scattering plane. The target polarization direction is specified by the angles $(\theta^*, \phi^*)$ in this coordinate system.

The kinematic factors $v_K$ are defined as follows:

$$v_L = (\frac{Q^2}{q^2})^2$$

$$v_T = \frac{1}{2}(\frac{Q^2}{q^2}) + \tan^2\frac{\theta}{2}$$

$$v_{TT} = -\frac{1}{2}(\frac{Q^2}{q^2})$$

$$v_{TL} = -\frac{1}{\sqrt{2}}(\frac{Q^2}{q^2})\sqrt{(\frac{Q^2}{q^2}) + \tan^2\frac{\theta}{2}}$$

$$v_{T'} = \tan\frac{\theta}{2}\sqrt{(\frac{Q^2}{q^2}) + \tan^2\frac{\theta}{2}}$$

$$v_{TL'} = -\frac{1}{\sqrt{2}}(\frac{Q^2}{q^2})\tan\frac{\theta}{2}$$

In order to display the sensitivity of the quasielastic asymmetry to the neutron form factors, it is useful to consider the special case of elastic scattering from the nucleon.

The spin-dependent asymmetry for the nucleon is expressible in terms of the electric and magnetic form factors as

$$A_{\vec{e}\vec{N}} = -\frac{2\tau v_{T'} \cos\theta^* G_M^2(Q^2) - 2\sqrt{2\tau(1+\tau)} v_{TL'} \sin\theta^* \cos\phi^* G_M(Q^2) G_E(Q^2)}{(1+\tau) v_L G_E^2 + 2\tau v_T G_M^2}. \quad (5)$$

Simple estimates of the expected asymmetries for quasielastic scattering from $^3$He can be obtained by using this expression multiplied by the ratio of neutron to $^3$He cross sections (spin-independent):

$$A_{He} \simeq A_{\vec{e}\vec{N}} \cdot \frac{\sigma_n}{\sigma_{He}}. \quad (6)$$

This expression is generally used in this proposal for the estimates of asymmetries.

The corrections to the above picture to account for the nuclear structure of $^3$He have been calculated by Blankleider and Woloshyn[10] and studied in further detail by Friar, et al.[11] The asymmetry for $\vec{q}$ perpendicular to the target spin is predominantly due to the neutron electric form factor. The major effect of the $^3$He nucleus is a dilution of the asymmetry due to the contribution of the protons to the unpolarized cross section and a smearing of the quasielastic strength due to the momentum distribution of the nucleons in the nucleus. In addition, small components of the $^3$He wave function in which the protons are polarized contribute $\sim$ 15% to the asymmetry in the region of momentum transfer proposed here. One should also consider the possibility that processes not included in these calculations can diminish the expected sensitivity to the neutron form-factors. The inclusive measurements proposed here should not be as sensitive to final state interactions (FSI) as exclusive measurements because there is an experimental integration over final states. One can expect that the theoretical treatment of the three-body continuum in nuclear physics will advance to the point where these issues can be quantitatively addressed during the next few years before the experiment is performed. Indeed, first calculations of the quasielastic response in the $A = 3$ system by solving the Fadeev equations in the continuum have recently been published.[12] The possible influence of meson exchange currents remains to be investigated theoretically. We expect our initial results at Bates at lower $Q^2$ will stimulate theoretical activity on these issues before the CEBAF experiments can be performed.

Measurements of the exclusive quasielastic reactions $(e, e'p)$ and $(e, e'n)$ will allow detailed testing of the nuclear effects (both final and initial states) mentioned above. Studying the $(e, e'n)$ reaction with $\vec{q}$ parallel to the target spin $\vec{S}$ will test the effect of final state interactions of the outgoing nucleon in the spin-dependent response (the neutron magnetic form factor and the initial neutron wave function are relatively well known a priori in this case). Note that we propose to perform this study over a very wide range of outgoing kinetic energies (0.2-1.0 GeV) so there is ample opportunity to test the theory. We will also study the asymmetry in $(e, e'p)$ at the same time; this asymmetry is identically zero for the dominant $S$-state ground state wave function when there are no final state effects. Therefore, after determination of the treatment of final state effects in the $(e, e'n)$ data we can confidently study the $S'$ and $D$ state effects on the spin dependent response (note that the proton form factors are well known). All of this information can then be

applied to the inclusive data in order to reliably extract the neutron form factors with good precision.

### Experimental Details

The experiments with polarized $^3$He targets are well-suited to the proposed CLAS in Hall B. Firstly, the luminosity is limited to $10^{33} - 10^{34}$ by beam depolarization of the target and the low density of the gas target[1]. Thus, it is important to utilize the large acceptance of the CLAS in order to obtain sufficient count rates. Secondly, many of these experiments require the detection of various final state hadrons which may populate a very large solid angle. Efficient data collection will require the very large acceptance of the CLAS. Finally, optically- pumped polarized $^3$He targets use small magnetic fields to orient the spins. This physics program *requires* that the spins be oriented in directions other than parallel to the beam (e.g., many measurements need the spin perpendicular to $\vec{q}$). Thus, the target region must be free of magnetic fields at the milligauss level. This is a very useful feature of the CLAS toroidal design. Note that we are using the entire region normally occupied by the region 1 drift chambers. These are to be removed from the CLAS for this experiment. The loss of momentum resolution is not a serious problem for the quasielastic experiments proposed here (see below). The other drift chambers are well shielded by the toroidal magnetic field so the background at the luminosity for this experiment ($1 \times 10^{33}/\mathrm{cm}^2$ /sec) should be very low.

## TARGET DESIGN

We have generated a preliminary design for the polarized target to be used in this experiment based on the assumption that we can transmit 60 $\mu$A of beam through the CLAS into the Hall B dump without significant background problems. This allows the most conservative polarized target design that will achieve the luminosity goal of $1 \times 10^{33}/\mathrm{cm}^2/\mathrm{sec}$. If the background level is too high with this amount of beam current (as determined by tests in advance of the experiment) we will then consider a more dense target. A factor of up to 20 can be achieved by cooling the gas still further with more complicated cryogenics. If more density is required we should be able to mechanically compress the gas to higher density. This technique is being developed at Mainz. Initial results are very encouraging and we expect that the technique will be further advanced by the Mainz group before CEBAF turns on.

The present design of the polarized target for the CLAS is shown in figure 2. It consists of two cells connected by a tube to allow diffusive transfer of gas from the glass cell where optical pumping takes place to the copper cell through which the beam passes. The target cell is 30 cm long, 2.54 cm in diameter and has thin ($\sim 5\mu$m) copper foil windows. (This is similar to the target we used at Bates which was 16 cm long.) The target cell will be maintained at a temperature of 77K by $LN_2$ in thermal contact with the cell through copper bars and braids. We only use 2 of the 6 CLAS segments so there is plenty of room available for these accessories as well as the pumping cell along with the gas feed for filling the target. The target pressure is 2 Torr which (for the central 12 cm of gas) yields a luminosity of $1 \times 10^{33}$ with 60 $\mu$A beam incident (we have used 20-40 $\mu$A

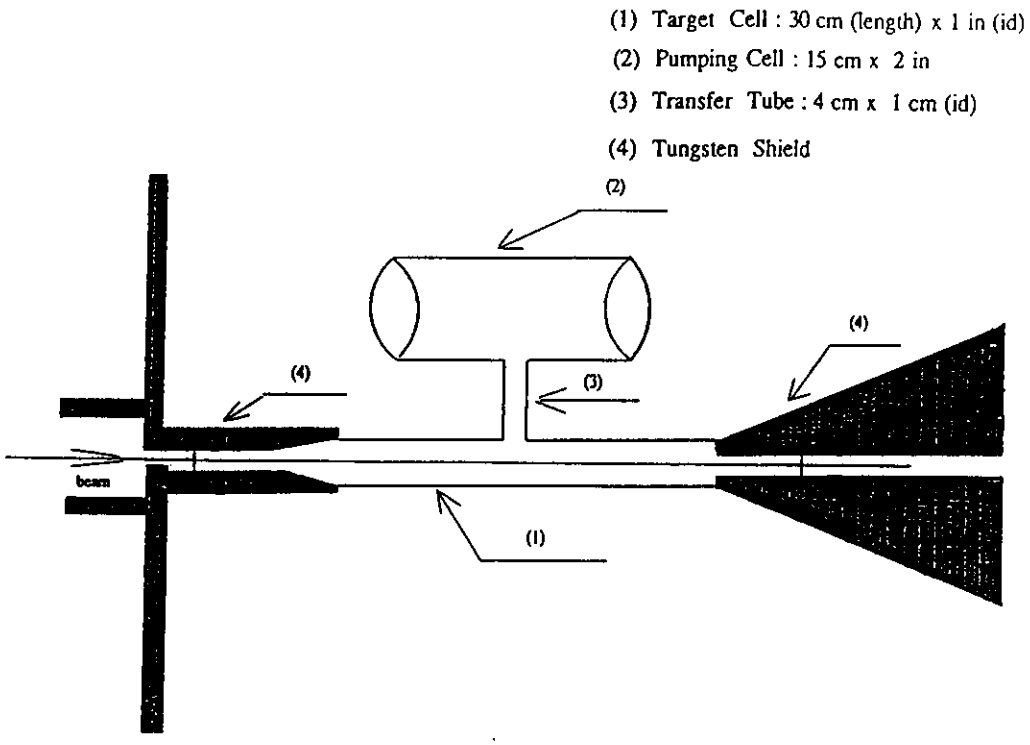


Fig. 2. Schematic diagram of polarized $^3$He target design.

at Bates). The expected power deposited in the target by the beam is less than 2 Watts which is a very modest thermal load at these temperatures.

In order to keep the count rate manageable in the CLAS we must collimate the end windows so that there is no direct line of sight to the detector system from either the entrance or exit window. This can be accomplished as shown in figure 2. The effective length of the target then varies from about 12 to 18 cm for electron scattering angles $15 - 45°$. The total acceptance for hadrons and electrons ranges from 15° to 90° with this collimation scheme.

The target is polarized by optical pumping with a LNA laser at 1.083 $\mu$. At present, we are able to achieve a pumping rate of $\sim 2 \times 10^{18}$ atoms polarized per second. This means that in the absence of depolarizing effects (discussed later), we could polarize the target proposed here in 30 seconds. A scheme for transmitting the laser light into the target is shown in figure 3.

The polarization of the target is measured by detecting the 667 nm light from the discharge in the pumping cell. The polarization of this light is proportional to the polarization of the $^3$He in the pumping cell. The target cell polarization (in the presence of beam) can be determined accurately from this measurement using auxiliary measurements of various time constants.[13] This was the technique utilized at Bates in previous experiments. The location of the 667 nm optical polarimeter is shown in figure 3.

The target will be polarized at 43° with respect to the beam direction. The holding field ($\sim$ 30 Gauss) is generated by Helmholtz coils with an 80 cm radius shown in figure 3. The current required in the coils is about 2700 Amp-turns.

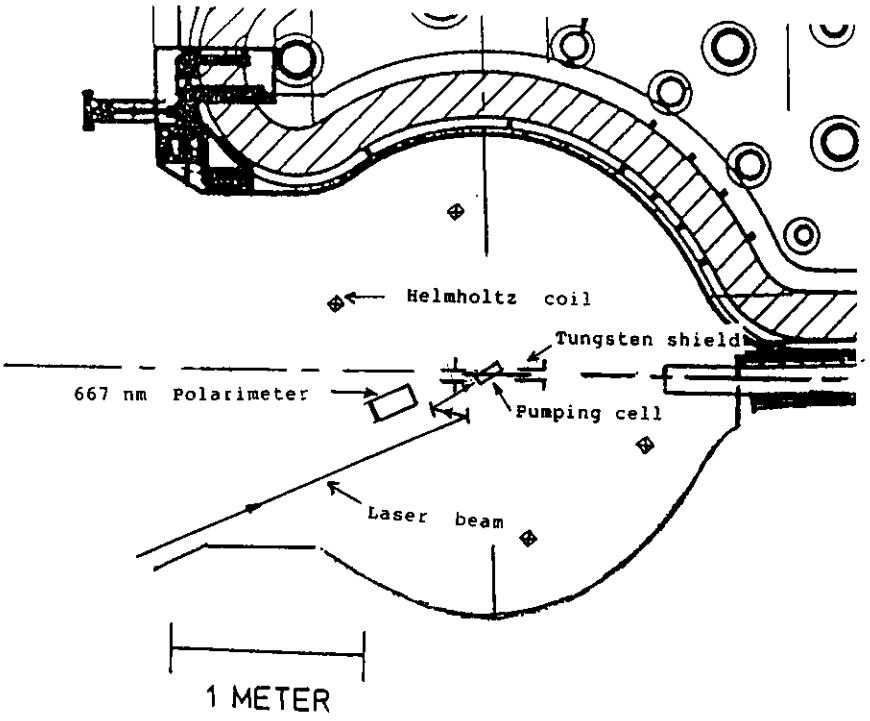


Fig. 3. Layout of laser, polarized target, Helmholtz coils, and optical polarimeter in the central cavity of the CLAS toroid.

## DEPOLARIZATION EFFECTS

We have carefully studied the various factors that can contribute to depolarization of the polarized $^3$He target. In the absence of beam, we expect the magnetic field gradients to be a major source of spin relaxation. (These present fluctuating transverse magnetic fields to the $^3$He atoms as they sample the target volume via thermal diffusion.) The relaxation rate due to gradients is given by the following formula:

$$\frac{1}{t_g} \equiv \frac{\langle v^2 \rangle}{3} \frac{\langle |\vec{\nabla} B_x|^2 + |\vec{\nabla} B_y|^2 \rangle}{B_0^2} \left( \frac{\tau_c}{1 + \omega_0^2 \tau_c^2} \right).$$

$B_0$ is the holding field, $\tau_c$ the mean time between atomic collisions, and $\omega_0 = \gamma B_0$ is the Larmor frequency for the magnetic field. For $^3$He the gyromagnetic ratio, $\gamma$, is 3.24 kHz/G. Schearer and Walters[14] measured the mean collision rate as a function of pressure at 300°K and determined that $\tau_c = (2.2 \pm 0.2) \times 10^{-7} p^{-1}$sec, where $p$ is the pressure in Torr. $\langle v^2 \rangle = 2kT/m$ is the average thermal velocity of the atoms.

We have computed the field gradients due to the CLAS toroid for two cases: a.) perfectly aligned toroidal coils, and b.) one coil misaligned by 1 mm. For case (a), the expression for the approximate field near the center of the toroid:

$$B_\phi = B_0 \, r^5 \cos 6\phi,$$
$$B_r = B_0 \, r^5 \sin 6\phi,$$
$$B_z = 0.$$

was used with $B_0 = 0.824$ Gauss as determined by a high precision numerical calculation of the toroidal field. In this case, we find the target relaxation time is predicted to be 8587 sec., dominated in fact by gradients due to the Helmholtz coils. For case (b), we find that a good approximation is obtained for a misaligned coil by adding a quadrupole moment at the coil position consisting of a dipole to cancel the coil contribution to first order and another identical dipole displaced by the misalignment distance of 1 mm. This accurately simulates the gradients at the toroid center as computed by brute force numerical calculation. The resulting relaxation time with the misaligned coil is 3300 sec. Therefore, all of these gradients produce relaxation times much longer than the projected pumping time of 30 sec (quoted above) and have a negligible effect on the degree of polarization obtained.

At a temperature of 77K the sticking time of $^3$He to the target cell walls will begin to cause some spin relaxation. This effect is much more severe at lower temperatures where we must coat the walls with Ar or $N_2$ to avoid large reductions in polarization. However, for the target we employed at Bates the relaxation time at 77K was about 500 sec, and we expect a similar result here. This is still significantly longer than the 30 sec. pump-up time.

Beam-induced depolarization is a much more significant effect. Based on results obtained in our previous runs at Bates, we expect that 60 $\mu$A of beam on the target proposed here would cause a relaxation time of about 150 sec. resulting in about a 20% reduction in the polarization (relative to the case with no beam). Since we anticipate about 55% polarization without beam, this implies we can expect at least 40% polarization in the presence of 60 $\mu$A of beam. This type of effect was easily corrected for in the experiments at Bates by carefully studying the time constants of the 2-cell system under various conditions. Using the optical monitor of the polarization in the pumping cell, we expect to have a continuous measure of the target cell polarization with better than 5% accuracy. (The average polarization in the target cell is a very accurate representation of the polarization of atoms within the beam path. For a beam radius of 1 mm, we find that the time for an atom to diffuse to the target wall is about 8 msec whereas it would take 5 sec to depolarize the atoms in the beam path in the absence of diffusive mixing. Therefore, the polarization in the target cell is well-mixed and uniform at all times.)

## BACKGROUND

We have considered background events from two sources: beam halo and multiply scattered electrons in the entrance foil interacting in the downstream endwindow collimator. According to a calculation of beam halo due to multiple scattering in the vacuum of the accelerator and beam transport system by G. Kraft (CEBAF), the fraction of beam particles outside of 1 cm radius is about $5 \times 10^{-9}$. Taking 1 radiation length of collimator or target cell material ($\sim$ 13 g/cm$^2$) compared to the $^3$He target thickness of $1.5 \times 10^{-5}$g/cm$^2$ implies a maximum of less than 1% expected background from halo. (Recall that at Bates we experienced about 10% background, but the CEBAF beam will have much higher quality.) Particles scattered in the end window and then the downstream collimator were simulated with GEANT, and we find that the rate of particles above 10 MeV escaping the collimator will be about 100 kHz. This implies that less than 10% of our events will contain a low energy background particle from the downstream collimator. They should be easily identifiable and eliminated from the data. As mentioned above, background from the beam dump is difficult to predict, so we request some test time early in the CLAS commissioning phase to study it.

## KINEMATICS AND PARTICLE DETECTION

We have assumed 2.5 GeV incident electron beam with 50% polarization. We anticipate using primarily 2 segments of the CLAS with shower counter implemented from 15° to 45° for electron identification. The very high $E'$ for quasielastic kinematics implies a very small pion contamination so the shower counter should be sufficient for electron identification. A single electron with energy above 1 GeV will trigger the system. We expect that the total trigger rate will be of order 100 Hz.

Of course, the "magic angle" where $\vec{q}$ is perpendicular to the target spin is only approximately maintained over this range of electron scattering angles. However, by considering the range of azimuthal angles for a sector of the CLAS the magic condition is approximately satisfied at every $\theta$. Thus, one can simultaneously measure the asymmetry corresponding to the neutron electric form factor over a wide range of $\theta$ and therefore over a wide range of $Q^2$. Of course, the rate drops off as $\theta$ increases so the statistical precision is less at higher $Q^2$.

Coincident protons and neutrons can be detected through the angular range 15°-90° with momenta greater than about 0.5 GeV/c. The neutron detection efficiency is expected to be about 40% at angles less than 45° (using the shower counter) and about 5% at larger angles (using the TOF scintillators).

The momentum resolution of the CLAS in this configuration will be typically 2% with angular resolution of about 0.1°. Thus the $\vec{q}$ direction can be determined to a fraction of a degree. The resolution in $Q^2$ will be better than 3%. For $(e, e'p)$ experiments, the resolution in the missing momentum $(\vec{p}_p - \vec{q})$ is estimated to be about 20-40 MeV/c.

**Table 1**
Quasielastic Kinematics.

| $\theta_e$ | $\frac{Q^2}{(\mathrm{GeV/c})^2}$ | $\frac{\mathrm{Rate}}{(\mathrm{Hz})}$ | $\theta_q$ | $\frac{\lvert\vec{q}\rvert}{(\mathrm{GeV/c})}$ | $\Delta\theta_{N-q}$ |
|---|---|---|---|---|---|
| 15° | 0.39 | 12 | 64° | 0.66 | 13° |
| 18° | 0.54 | 5.8 | 60° | 0.79 | 11° |
| 21.5° | 0.73 | 2.7 | 55° | 0.94 | 9° |
| 25.7° | 0.98 | 1.2 | 50° | 1.11 | 8° |
| 30.7° | 1.27 | 0.53 | 45° | 1.32 | 7° |
| 36.5° | 1.61 | 0.23 | 40° | 1.53 | 6° |
| 43.3° | 1.97 | 0.10 | 34° | 1.76 | 5° |

The proposed quasielastic kinematics are listed in table 1. Note that the coincident nucleons are typically located in a narrow cone of angle

$$\Delta\theta_{N-q} = \frac{0.15\mathrm{GeV/c}}{|\vec{q}|} \lesssim 13°.$$

The inclusive quasielastic rates are for a luminosity of $1 \times 10^{33}$ /cm$^2$ /sec and one segment (1/6) of the CLAS. (We will, however, accept electron triggers from two opposite segments centered in the plane formed by the beam momentum and target spin vectors.)

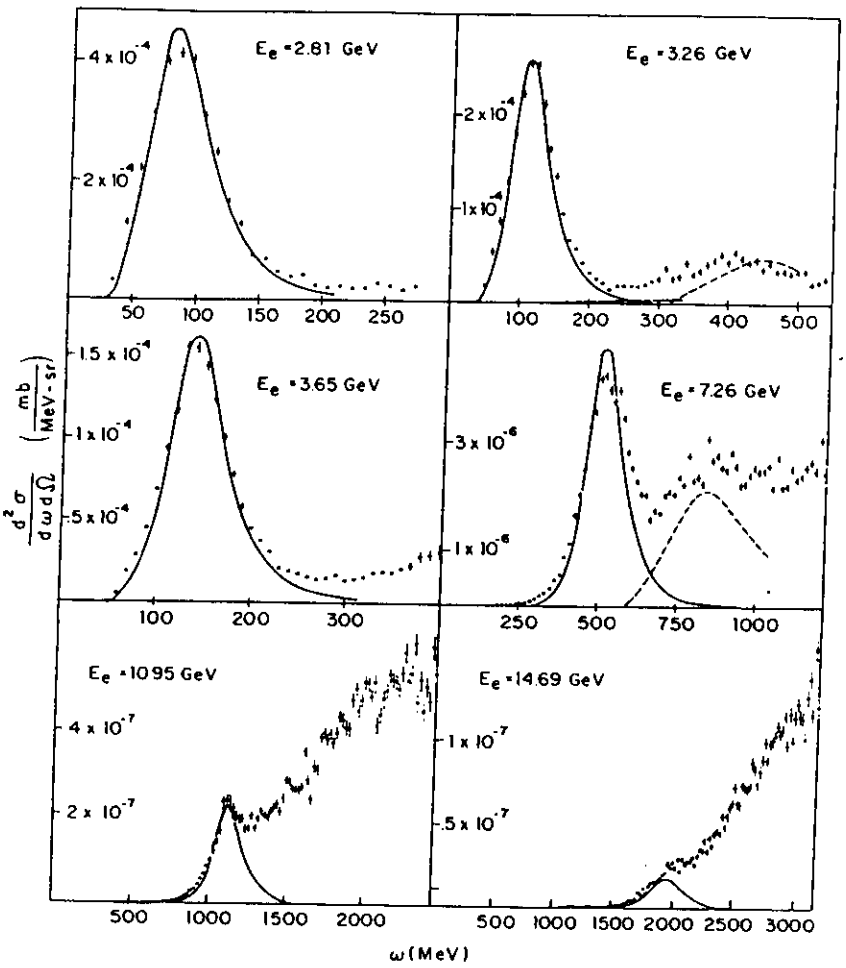


**Inclusive cross sections for $\theta = 8°$ compared with QFS calculation based on Faddeev wave function. The dashed line is the contribution due to $\Delta(1236)$ excitation (Ref. 21), the broken-dash line is the meson-exchange current contribution (Ref. 22).**

Fig. 4. Inclusive quasielastic electron scattering data on $^3$He from SLAC.

SLAC data[15] for inclusive quasielastic scattering in the $Q^2$ range relevant to this experiment are shown in figure 4. For $Q^2 < 2$ (GeV/c)$^2$ one sees a clear quasielastic peak that is well described by a spectral function based on a Fadeev calculation. At the larger momentum transfers ($Q^2 \sim 2$ (GeV/c)$^2$), one may need to require a nucleon in coincidence to obtain a clear quasielastic signal. The full width (FWHM) of the peak varies from 90-160 MeV in the range of momentum transfers $0.5 \leq Q^2 \leq 2$ (GeV/c)$^2$. The expected resolution (FWHM) of the CLAS system without the region 1 drift chambers will vary from 38 to 110 MeV over this range. Figure 5 shows simulated quasielastic spectra generated by $y$-scaling over the kinematic range of the proposed experiment along with the expected CLAS resolution. One can see that the expected resolution is only a fraction of the width of the quasielastic peak in each case.

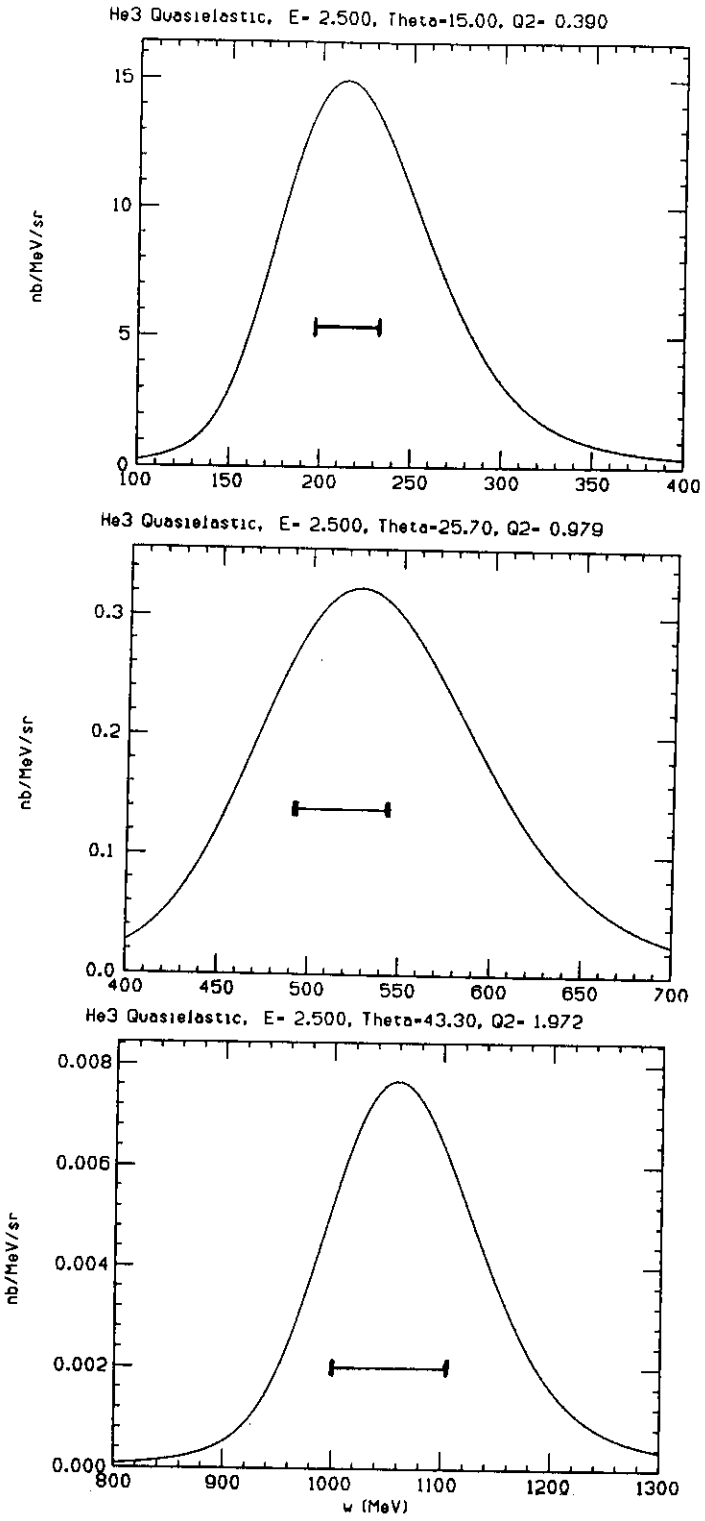


Fig. 5. Calculated quasielastic peaks at kinematics for the proposed experiment. The FWHM resolution of the CLAS at each setting is indicated by a horizontal bar.

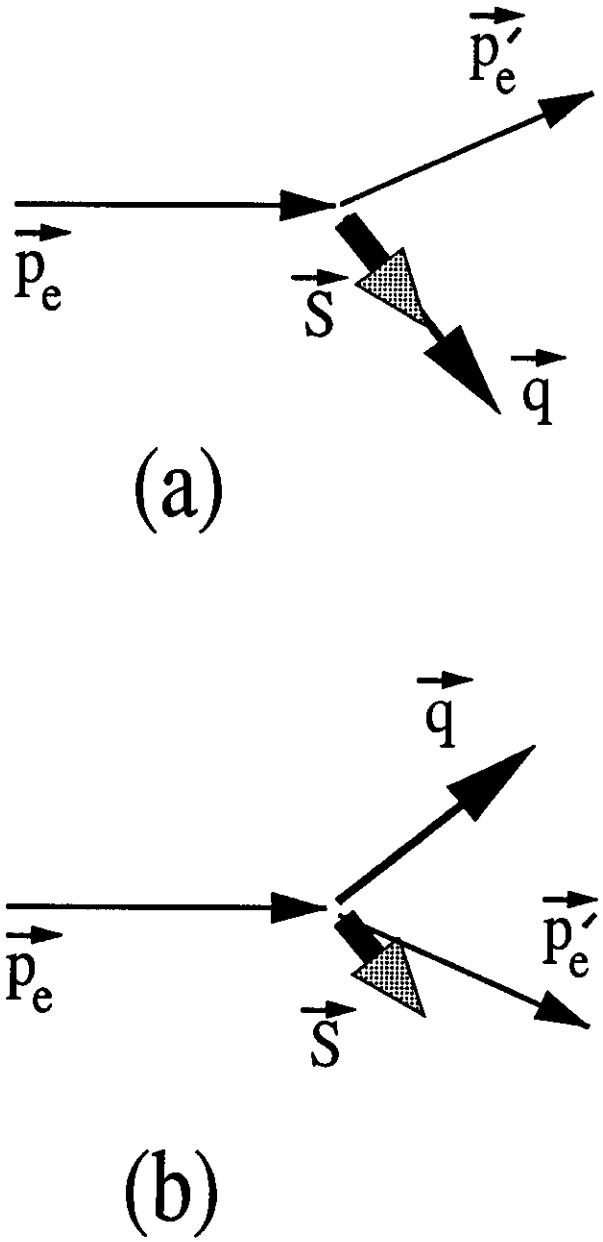


Fig. 6. Kinematic vectors for the inclusive $(e, e')$ experiments with (a) $\vec{q} \| \vec{S}$ and (b) $\vec{q} \perp \vec{S}$.

We will discuss 4 experiments in succession based on the data acquired (all simultaneously) during a 30 day run with this setup:

1.) inclusive quasielastic $(e, e')$ with $\vec{q} \| \vec{S}$,
2.) inclusive quasielastic $(e, e')$ with $\vec{q} \perp \vec{S}$,
3.) quasielastic $(e, e'p)$ for both $\vec{q} \| \vec{S}$ and $\vec{q} \perp \vec{S}$, and
4.) quasielastic $(e, e'n)$ for both $\vec{q} \| \vec{S}$ and $\vec{q} \perp \vec{S}$.

Figure 6a shows the relevant orientation of various kinematic vectors for experiment type (1). This experiment is primarily sensitive to the neutron magnetic form factor, and the asymmetries, indicated as $A_{\|}$ in table 2 are correspondingly large. The projected statistical uncertainty in the asymmetry is also listed in table 2 as $\Delta A$. We have assumed 40% target polarization and 50% beam polarization in these and the other estimates in this proposal.

**Table 2**
Inclusive Asymmetries.

| $\theta$ | $Q^2$ | $A_{\|}(\%)$ | $A_{\perp}(\%)$ | | $\Delta A(\%)$ |
|---|---|---|---|---|---|
| | $(\mathrm{GeV/c})^2$ | | $A_{\mathrm{Galster}}$ | $A_{G-K}$ | |
| 15° | 0.39 | 0.60 | 0.36 | 0.43 | 0.03 |
| 18° | 0.54 | 0.83 | 0.43 | 0.56 | 0.04 |
| 21.5° | 0.73 | 1.1 | 0.49 | 0.71 | 0.06 |
| 25.7° | 0.98 | 1.5 | 0.41 | 0.86 | 0.10 |
| 30.7° | 1.27 | 1.9 | 0.27 | 1.0 | 0.16 |
| 36.5° | 1.61 | 2.4 | 0.16 | 1.1 | 0.22 |
| 43.3° | 1.97 | 3.0 | −0.09 | 1.2 | 0.34 |

Figure 6b shows the geometry corresponding to experiment type 2 which is sensitive to the neutron's electric form factor. The asymmetries corresponding to the Galster parametrization ($A_{Galster}$) and Gari-Krumpelmann ($A_{G-K}$) are listed in table 2. The uncertainty expected in this measurement is also given by the quantity $\Delta A$ in table 2. Figure 7 shows the expected statistical uncertainty for the extraction of $G_E^n$ from these data in a 30 day run.

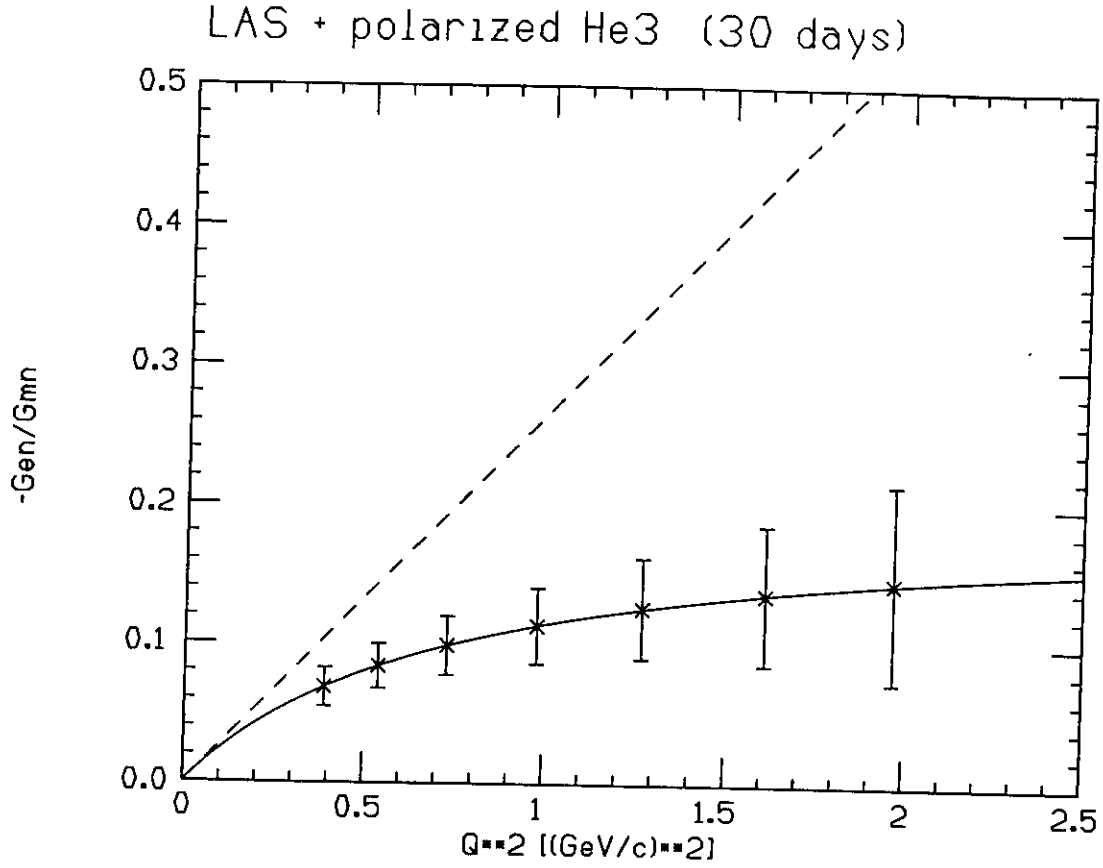


Fig. 7. Attainable statistical precision for a single 30 day run for the neutron electric form-factor as a function of the momentum transfer. The ratio to the magnetic form-factor is plotted, and the solid line is a standard parametrization used in Galster *et al.*, while the dashed line is the recent prediction of Gari and Krumpelmann.

Figure 8 shows the kinematic geometry for experiment type 3. This experiment will test the spin contribution of protons from the $S'$ and $D$ states in the $^3$He wave function. The proton asymmetry for coincident protons with smaller missing momentum $p_m$ is more sensitive to the $S'$ contribution whereas those with large $p_m$ will show more sensitivity to the $D$ state. The energy dependence will test the final state interaction contributions. Table 3 lists the rates and asymmetries for the $(e, e'p)$ experiment. Notice that the asymmetries are small and that the measurements will be more significant (statistically) at lower $Q^2$.

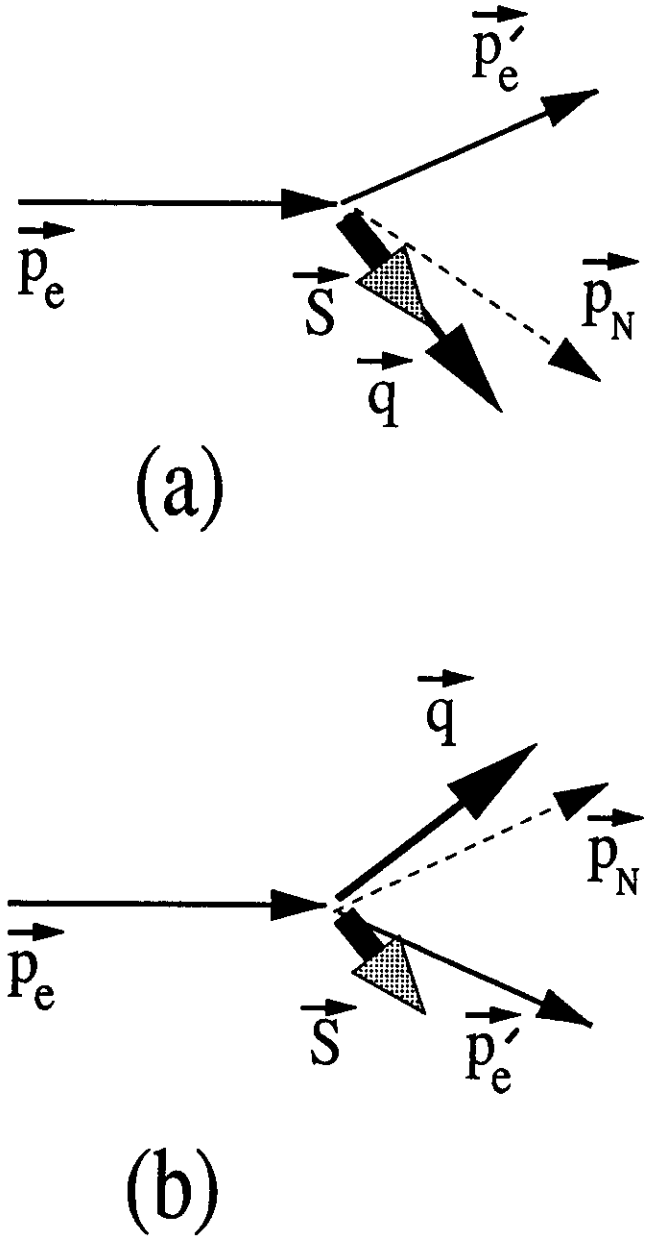


Fig. 8. Kinematics for $(e, e'N)$ and experiments with (a) $\vec{q} \| \vec{S}$ and (b) $\vec{q} \perp \vec{S}$.

**Table 3**
$(e, e'p)$ Rates and Asymmetries

| $\theta$ | $\frac{Q^2}{(\mathrm{GeV/c})^2}$ | $\frac{\mathrm{Rate}}{(\mathrm{Hz})}$ | $A_\parallel(\%)$ | $A_\perp(\%)$ | $\Delta A(\%)$ |
|---|---|---|---|---|---|
| 15° | 0.39 | 7.9 | 0.12 | −0.28 | 0.04 |
| 18° | 0.54 | 4.0 | 0.17 | −0.23 | 0.05 |
| 21.5° | 0.73 | 1.9 | 0.22 | −0.21 | 0.08 |
| 25.7° | 0.98 | 0.87 | 0.30 | −0.14 | 0.12 |
| 30.7° | 1.27 | 0.38 | 0.38 | −0.09 | 0.20 |
| 36.5° | 1.61 | 0.16 | 0.48 | −0.04 | 0.26 |
| 43.3° | 1.97 | 0.07 | 0.60 | −0.02 | 0.40 |

Figure 8 also shows the kinematics for experiment type 4. This $(e, e'n)$ experiment will test the final state interaction contribution to the asymmetry as well as provide additional information on the neutron form factors from a subset of the data. In table 4 we see that the expected asymmetries are quite large for both $\vec{q} \| \vec{S}$ and $\vec{q} \perp \vec{S}$. Note that, at large $Q^2$ where we expect good neutron detection efficiency, there will be excellent sensitivity to $G_e^n$ in the measured values of $A_\perp$.

**Table 4**
$(e, e'n)$ Rates and Asymmetries

| $\theta$ | $Q^2$ | Rate | $A_\parallel(\%)$ | $A_\perp(\%)$ | | $\Delta A(\%)$ |
|---|---|---|---|---|---|---|
| | $(\mathrm{GeV/c})^2$ | $(\mathrm{min}^{-1})$ | | (Galster) | $G-K$ | |
| 15° | 0.39 | 2.6 | 6.0 | 3.6 | 4.3 | 0.50 |
| 18° | 0.54 | 1.6 | 7.1 | 3.7 | 4.8 | 0.59 |
| 21.5° | 0.73 | 0.9 | 8.6 | 3.8 | 5.5 | 0.80 |
| 25.7° | 0.98 | 0.5 | 10.1 | 2.8 | 5.9 | 1.2 |
| 30.7° | 1.27 | 1.7 | 11.8 | 1.7 | 6.3 | 0.68 |
| 36.5° | 1.61 | 0.8 | 13.9 | 0.93 | 6.4 | 0.39 |
| 43.3° | 1.97 | 0.4 | 16.4 | −0.49 | 6.5 | 1.3 |

SYSTEMATIC ERRORS

Based on our previous experience at Bates, we expect that the measurement of beam and target polarizations will be the dominant systematic errors. These were both limited to about 10% at Bates. Improvements we have made in our target polarization monitoring capability should allow $\lesssim 5\%$ measurement of the target polarization. In addition, CW beam will allow coincident detection of both electrons in a Moller polarimeter at CEBAF. This will eliminate the major problem of inelastic nuclear background we encountered with the beam polarimeter at Bates. We also expect that 5% measurement of beam polarization at CEBAF should be relatively straightforward.

It is also important to install non-intrusive (i.e., cavity-type) beam position monitors upstream of the target which are capable of detecting any helicity correlated beam movement. This capability is necessary to check that such effects (which may cause false asymmetries) are small enough that significant systematic errors to not result. This will, of course, be a necessary ingredient of any polarized beam experiment at CEBAF.

### Resources Required

As stated above, these measurements rely on the CLAS (with region 1 drift chambers removed) and require that there be a field-free region at the target position. We only require two opposing sextants of the CLAS to be instrumented for this experiment. One should note that, as opposed to measuring cross sections, the measurement of spin dependent asymmetries does not require detailed understanding of the acceptance of a device like the CLAS.

Availability of a high-intensity ($\lesssim 60\ \mu$A) polarized ($\sim 50\%$) electron beam at 2.5 GeV and a suitable polarimeter for monitoring polarization are also required. We would construct the polarized $^3$He target at Caltech. This will require about 1 year lead time.

### Beam Request

A total of 30 days running time with one week of tune-up are requested to perform these measurements. We will need about one day of test time early in the CLAS commissioning phase to assess the backgrounds from the beam dump with a high intensity (60 $\mu$A) beam.

## References


[1] R. G. Milner, R. D. McKeown, and C. E. Woodward, Nucl. Instr. Meth. **A257**, 286 (1987); and Nucl. Instr. Meth. **A274**, 56 (1989).

[2] C. E. Woodward *et al.*, Phys. Rev. Lett. **65**, 698 (1990); C. E. Jones-Woodward *et al.*, Phys. Rev. **C44**, R571 (1991).

[3] T. W. Donnelly and A. S. Raskin, Annals of Physics **169**, 247(1986).

[4] T.W. Donnelly, Proceedings of Workshop in Electronuclear Physics with Internal Targets, SLAC January 1987, p. 28.

[5] S. Galster *et al.*, Nucl. Phys. **B32**, 221(1971); S. Platchkov *et al.*, Nucl. Phys. **A510**, 740 (1990).

[6] M. Gari and W. Krumpelmann, Z. Phys. **A322**, 689 (1985); Phys. Lett. **B173**, 10 (1986).

[7] R. D. McKeown and R. G. Milner, Research Program at CEBAF, p. 12-45(1985).

[8] H. J. Lipkin and T. -S. H. Lee, Physics Letters **B183**, 22(1987).

[9] R. G. Milner and T.W.Donnelly, Phys. Rev. **C37**, 870 (1988)

[10] B. Blankleider and R. M. Woloshyn, Phys. Rev. **C29**, 538(1984).

[11] J. Friar, *et al.*, Phys. Rev. **C42**, 2310 (1990).

[12] E. Van Meijgaard and J. A. Tjon, Phys. Lett. **B228**, 307(1989).

[13] C. E. Jones, Caltech Ph.D. thesis, unpublished.

[14] L. D. Schearer and G. K. Walters, Phys. Rev. **139**, A1398 (1965).

[15] D. Day *et al.*, Phys. Rev. Lett. **43**, 1143 (1979).